A R C H I V E O F M E C H A N I C A L E N G I N E E R I N G

Volume 68 2021 Number 1

DOI: 10.24425/ame.2020.131706

Key words: static analysis, functionally graded plates, Winkler-Pasternak foundation, physical neutral surface, four-variable refined theory

Van-Loi Nguyen [1], Minh-Tu Tran [1], Van-Long Nguyen [1], Quang-Huy Le [2]

Static behaviour of functionally graded plates resting on elastic foundations using neutral surface concept

In this study, static behaviors of functionally graded plates resting on Winkler-Pasternak elastic foundation using the four-variable refined theory and the physical neutral surface concept is reported. The four-variable refined theory assumes that the transverse shear strain has a parabolic distribution across the plate's thickness, thus, there is no need to use the shear correction factor. The material properties of the plate vary continuously and smoothly according to the thickness direction by a power-law distribution. The geometrical middle surface of the functionally graded plate selected in computations is very popular in the existing literature. By contrast, in this study, the physical neutral surface of the plate is used. Based on the four-variable refined plate theory and the principle of virtual work, the governing equations of the plate are derived. Next, an analytical solution for the functionally graded plate resting on the Winkler-Pasternak elastic foundation is solved using the Navier's procedure. In numerical investigations, a comparison of the static behaviors of the functionally graded plate between several models of displacement field using the physical neutral surface is given, and parametric studies are also presented.

1. Introduction

In recent years, together with the advancement in material sciences, a new kind of material is proposed called the functionally graded materials (FGMs). This type of material consists of two ceramic and metal constituents, thus, it has many advantages such as high strength, toughness, and good capacity of corrosion and thermal resistance, etc. [1–3]. Besides, material properties of the functionally

✉ Van-Loi Nguyen, e-mails: loinv@nuce.edu.vn, nguyenvanloi.n.v@gmail.com

[1]Department of Strength of Materials, National University of Civil Engineering, Hanoi, Vietnam; ORCIDs: V-L.N: 0000-0002-8801-3433; M-T.T.: 0000-0002-2208-3463.

[2]Department of Highway Engineering, Faculty of Civil Engineering, University of Transport Technology, Hanoi, Vietnam.

graded (FG) structure can vary smoothly and continuously according to its one or more directions, hence, this material may correct the disadvantages of the laminated composite material in terms of peeling laminate off and focusing stresses. Recently, functionally graded structures have been widely applied in various industries such as civil engineering, aerospace engineering, nuclear, automotive, mechanics [4–9].

Interestingly, studies on the static and dynamic behaviors of the plate structures have always attracted many researchers in recent years. Until now, several models of plate theories for static and dynamic behaviors have been proposed. The classical plate theory (CPT) based on the Kirchhoff's assumptions is the simplest, but is suitable only for the thin plates due to ignoring the transverse shear deformation effects [2, 10]. To overcome the limitation of the classical plate theory, there are some models of the shear deformation plate theories introduced. For example, the first-order shear deformation plate theory (FSDT) including the effect of the transverse shear deformation was proposed. However, this plate theory needs an additional assumption that transverse shear deformation strain through the thickness of the plate is constant [11]. This phenomenon causes that the FSDT theory doesn't satisfy the zero traction boundary conditions on the bottom and the top surfaces of the plate. In the next stage, the higher-order shear deformation plate theories (HSDTs) were proposed to correct the inconvenience of the FSDT theory. Studies on static behaviors and free vibration of the FG plates using the HSDTs maybe be found in the literature [6, 12–16]. Besides, investigations of static and dynamic behaviors of the FG plates on elastic foundations have also been getting attention. A series of studies on the functionally graded plates resting on elastic foundation has been carried out. However, most of these studies use the geometrical middle surface for calculations. Actually, the geometrical middle surface does not coincide with the physical neutral surface of the FG plate, due to the material properties of functionally grade plate are not symmetric throughout its thickness, they can be found in several works on static and dynamic characteristics of the FG plate based on the neutral surface concept in the existing literature [17–21]. In many studies, Zhang and Zhou [17], Thai and Uy [22], Khalfi et al. [23], Bellifa et al. [24] showed that the stretching – bending coupling is equal to zero when the reference surface selected is the neutral surface of FG plate. Therefore, the equations and calculations for the FG plate are simpler than those of other approaches.

Based on the above reviews, this study focuses on static analysis of the functionally graded plates resting on the Winkler-Pasternak elastic foundation using the four-variable refined plate theory (RPT) together with the physical neutral surface concept. By using Navier's procedure, an analytical solution for the simply supported FG plate resting on the elastic foundation is found. Especially, in this paper, comparisons of static behaviors (i.e., deflection and stress components) of several models of displacement field using neutral surface concept are studied and some useful comments are given.

This paper has four sections and they will be presented in the following. In section 2, theoretical formulations used to derive the governing equations of the

plate resting on elastic foundation, and a Navier's procedure for static analysis of the FG plate will be presented. In section 3, some comparisons to show the influences of several models of displacement field on static behaviors (i.e., deflection, stress results) of the FG plate will be given. Next, some effects of several relevant factors (i.e., fraction volume index, geometric dimensions, and elastic foundation) on the deflection and stress components will be also presented in section 3. In the last section, some conclusions are given.

2. Theoretical formulations and solution methodology

2.1. Materials, kinematic and constitutive relations

A rectangular plate made of functionally graded material in the reference coordinate system (x, y, z) is considered as shown in Fig. 1a. Symbols a, b, h stand for length, width, and thickness of the plate, respectively. Symbols z and z_{ns} denote the distances according to thickness direction from a certain point to the geometrical middle surface and neutral surface of the FG plate as shown in Fig. 1b. The material properties of the FGM (Young's modulus, mass density), except the Poisson's ratio are assumed to be graded through the thickness direction of the plate according to a simple power-law as follows [2, 23, 25]:

$$P(z) = P_m + (P_c - P_m)\left(\frac{z}{h} + \frac{1}{2}\right)^p = P_m + (P_c - P_m)\left(\frac{z_{ns} + z_0}{h} + \frac{1}{2}\right)^p, \quad (1)$$

where P_m and P_c are the material properties of the metal and ceramic constituents, respectively; p is the volume fraction index and the parameter z_0 is the shift of the neutral surface from the physical middle surface of the FG plate. The variation of material properties through the thickness of the plate with various volume fraction index is illustrated in Fig. 2.

The bottom surface is metal-rich and the top surface is ceramic-rich, as shown in Fig.1b. As we know, besides the concept of geometric middle surface, there

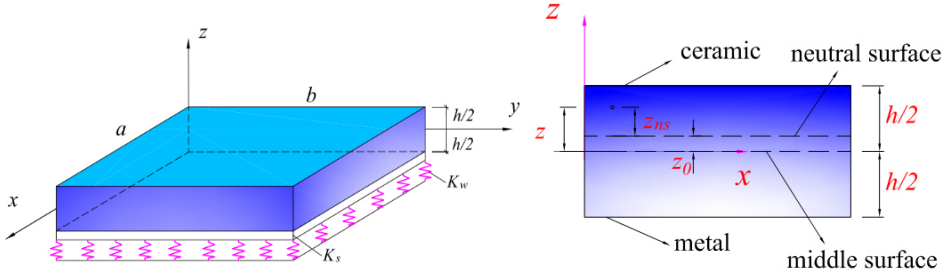

(a) A functionally graded plate resting on the Winkler–Pasternak foundation

(b) The geometrical middle surface and neutral surface of the FG plate

Fig. 1. Schematic of a functionally graded plate resting on the Winkler–Pasternak foundation

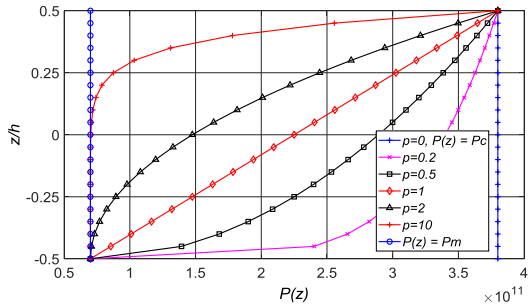

Fig. 2. The variation of material properties through the thickness of the plate

is the concept of physical neutral surface, in which normal stresses are zero. The position of the neutral surface can be determined by [23, 25]:

$$z_0 = \frac{\int_{-h/2}^{h/2} E(z) z \, \mathrm{d}z}{\int_{-h/2}^{h/2} E(z) \, \mathrm{d}z}, \tag{2a}$$

$$z^* = \frac{\int_{-h/2}^{h/2} E(z) f(z) \, \mathrm{d}z}{\int_{-h/2}^{h/2} E(z) \, \mathrm{d}z}. \tag{2b}$$

where $E(z)$ is Young's modulus of FGM, and the function $f(z)$ is defined in bellow, Eq. (3). Based on the physical neutral surface concept and the four-variable refined plate theory, the displacement fields of the FG plate are assumed to be in the form [23, 25, 26]:

$$\begin{aligned} u(x,y,z) &= u_0(x,y) - (z - z_0)\frac{\partial w_b}{\partial x} - \left[f(z) - z^*\right]\frac{\partial w_s}{\partial x}, \\ v(x,y,z) &= v_0(x,y) - (z - z_0)\frac{\partial w_b}{\partial y} - \left[f(z) - z^*\right]\frac{\partial w_s}{\partial y}, \\ w(x,y,z) &= w_b(x,y) + w_s(x,y). \end{aligned} \tag{3}$$

where $f(z) = -\frac{1}{4}z + \frac{5}{3}\frac{z^3}{h^2}$; u_0, v_0 is the displacement components of a point located on the neutral surface in the x- and y-directions, respectively; The total transverse

displacement of the midplane of the plate is w, symbols w_b and w_s are the bending and shear components of mid-plane transverse displacement, respectively.

In this study, two models of the displacement field for the higher-order shear deformation theory are considered and compared as follows:

- **Model 1 (M1):** $z_0 \neq 0$, $z^* = 0$. In this case, the reference surface is the neutral surface of the FG plate, displacement fields based on the expressions of Bousahla et al. [18] and Khalfi et al. [23].
- **Model 2 (M2):** $z_0 \neq 0$, $z^* \neq 0$. In this model, the reference surface is the neutral surface of the FG plate, however, displacement fields based on the expressions of Zhang [21], Shahverdi and Barati [25].

It is assumed that nonlinear components of the strain field are ignored in this study. The linear strains of the FG plate can be defined by [21, 25]:

$$\begin{Bmatrix} \varepsilon_x \\ \varepsilon_y \\ \gamma_{xy} \end{Bmatrix} = \begin{Bmatrix} \varepsilon_x^0 \\ \varepsilon_y^0 \\ \gamma_{xy}^0 \end{Bmatrix} + (z - z_0) \begin{Bmatrix} k_x^b \\ k_y^b \\ k_{xy}^b \end{Bmatrix} + [f(z) - z^*] \begin{Bmatrix} k_x^s \\ k_y^s \\ k_{xy}^s \end{Bmatrix}, \tag{4a}$$

$$\begin{Bmatrix} \gamma_{yz} \\ \gamma_{xz} \end{Bmatrix} = g(z) \begin{Bmatrix} \gamma_{yz}^s \\ \gamma_{xz}^s \end{Bmatrix}. \tag{4b}$$

where

$$\varepsilon_x^0 = \frac{\partial u_0}{\partial x}, \quad k_x^b = -\frac{\partial^2 w_b}{\partial x^2}, \quad k_x^s = -\frac{\partial^2 w_s}{\partial x^2}, \tag{5a}$$

$$\varepsilon_y^0 = \frac{\partial v_0}{\partial y}, \quad k_y^b = -\frac{\partial^2 w_b}{\partial y^2}, \quad k_y^s = -\frac{\partial^2 w_s}{\partial y^2}, \tag{5b}$$

$$\gamma_{xy}^0 = \frac{\partial u_0}{\partial y} + \frac{\partial v_0}{\partial x}, \quad k_{xy}^b = -2\frac{\partial^2 w_b}{\partial x \partial y}, \quad k_{xy}^s = -2\frac{\partial^2 w_s}{\partial x \partial y}, \tag{5c}$$

$$\gamma_{yz}^s = \frac{\partial w_s}{\partial y}, \quad \gamma_{xz}^s = \frac{\partial w_s}{\partial x}, \tag{5d}$$

$$g(z) = 1 - f'(z) = \frac{5}{4} - 5\left(\frac{z}{h}\right)^2. \tag{5e}$$

The constitutive relation of the FG plate is given by:

$$\begin{Bmatrix} \sigma_x \\ \sigma_y \\ \sigma_{xy} \\ \sigma_{yz} \\ \sigma_{xz} \end{Bmatrix} = \begin{bmatrix} Q_{11} & Q_{12} & 0 & 0 & 0 \\ Q_{12} & Q_{22} & 0 & 0 & 0 \\ 0 & 0 & Q_{66} & 0 & 0 \\ 0 & 0 & 0 & Q_{44} & 0 \\ 0 & 0 & 0 & 0 & Q_{55} \end{bmatrix} \begin{Bmatrix} \varepsilon_x \\ \varepsilon_y \\ \gamma_{xy} \\ \gamma_{yz} \\ \gamma_{xz} \end{Bmatrix}, \tag{6}$$

with

$$Q_{11} = Q_{22} = \frac{E(z)}{1 - \upsilon^2}, \quad Q_{12} = \frac{\upsilon E(z)}{1 - \upsilon^2}, \quad Q_{44} = Q_{55} = Q_{66} = \frac{E(z)}{2(1 + \upsilon)}. \tag{7}$$

The force and moment resultants in the FG plate are defined by:

$$\left(\left\{\begin{array}{c} N_x \\ N_y \\ N_{xy} \end{array}\right\}, \left\{\begin{array}{c} M_x^b \\ M_y^b \\ M_{xy}^b \end{array}\right\}, \left\{\begin{array}{c} M_x^s \\ M_s^s \\ M_{xy}^s \end{array}\right\}\right) = \int_{-h/2}^{h/2} \left\{\begin{array}{c} \sigma_x \\ \sigma_y \\ \sigma_{xy} \end{array}\right\} (1,\ z - z_0,\ f(z) - z^*)\, \mathrm{d}z, \tag{8a}$$

$$\left\{\begin{array}{c} Q_{yz} \\ Q_{xz} \end{array}\right\} = \int_{-h/2}^{h/2} \left\{\begin{array}{c} \sigma_{yz} \\ \sigma_{xz} \end{array}\right\} g(z)\, \mathrm{d}z. \tag{8b}$$

The matrix form of the Eq. (8) can be written as follows:

$$\left\{\begin{array}{c} N \\ M^b \\ M^s \end{array}\right\} = \left[\begin{array}{ccc} A & B & B^s \\ B & D & D^s \\ B^s & D^s & H^s \end{array}\right] \left\{\begin{array}{c} \varepsilon \\ k^b \\ k^s \end{array}\right\}, \quad S = A^s \gamma, \tag{9}$$

where

$$\left\{\begin{array}{l} N = \left\{\begin{array}{cccc} N_x & N_y & N_{xy} \end{array}\right\}^t, \\ M^b = \left\{\begin{array}{cccc} M_x^b & M_y^b & M_{xy}^b \end{array}\right\}^t, \\ M^s = \left\{\begin{array}{cccc} M_x^s & M_y^s & M_{xy}^s \end{array}\right\}^t, \end{array}\right. \tag{10a}$$

$$\left\{\begin{array}{l} \varepsilon = \left\{\begin{array}{cccc} \varepsilon_x^0 & \varepsilon_y^0 & \gamma_{xy}^0, \end{array}\right\}^t \\ k^b = \left\{\begin{array}{cccc} k_x^b & k_y^b & k_{xy}^b \end{array}\right\}^t, \\ k^s = \left\{\begin{array}{cccc} k_x^s & k_y^s & k_{xy}^s \end{array}\right\}^t, \end{array}\right. \tag{10b}$$

$$S = \left\{\begin{array}{cccc} Q_{yz}^s & Q_{xz}^s \end{array}\right\}^t, \tag{10c}$$

$$\gamma = \left\{\begin{array}{cccc} \gamma_{yz} & \gamma_{xz} \end{array}\right\}^t, \tag{10d}$$

$$A^s = \left[\begin{array}{cc} A_{44}^s & 0 \\ 0 & A_{55}^s \end{array}\right], \tag{10e}$$

$$M = \left[\begin{array}{ccc} M_{11} & M_{12} & 0 \\ M_{12} & M_{22} & 0 \\ 0 & 0 & M_{66} \end{array}\right], \quad M = A, B, D, B^s, D^s, H^s\,. \tag{10f}$$

here, the coefficients A_{ij}, B_{ij}, D_{ij}, B^s_{ij}, D^s_{ij}, H^s_{ij}, A^s_{ij} are defined by:

$$\left\{A_{ij},\ B_{ij},\ D_{ij}\right\} = \int_{-h/2}^{h/2} \left\{1,\ (z-z_0),\ (z-z_0)^2\right\} Q_{ij}\,\mathrm{d}z,$$
$$(ij) = (11, 12, 22, 66), \tag{11a}$$

$$\left\{B^s_{ij},\ D^s_{ij},\ H^s_{ij}\right\} = \int_{-h/2}^{h/2} \left\{\left[f(z)-z^*\right],\ (z-z_0)\left[f(z)-z^*\right],\right.$$
$$\left.\left[f(z)-z^*\right]^2\right\} Q_{ij}\,\mathrm{d}z, \quad (ij) = (11, 12, 22, 66), \tag{11b}$$

$$A^s_{ij} = \int_{-h/2}^{h/2} g^2(z) Q_{ij}\,\mathrm{d}z \quad (ij) = (44, 55). \tag{11c}$$

2.2. Governing equations

To obtain governing equations of the functionally graded plate resting on the Winkler-Pasternak elastic foundation using the four-variable refined theory and the physical neutral surface concept, the principle of virtual work is applied. The analytical form of the principle of virtual work can be stated by:

$$\delta\left(U_p + U_f + \Omega\right) = 0, \tag{12}$$

where U_p, U_f and Ω are the strain energy of the FG plate, the potential energy due to the elastic foundation, and the potential energy due to the transverse applied load, respectively.

The strain energy of the FG plate can be given by [27]:

$$U_p = \frac{1}{2}\int_A \begin{pmatrix} N_x\varepsilon^0_x + N_y\varepsilon^0_y + N_{xy}\gamma^0_{xy} + M^b_x\kappa^b_x + \\ +M^b_y\kappa^b_y + M^b_{xy}\kappa^b_{xy} + M^s_x\kappa^s_x + M^s_y\kappa^s_y + \\ +M^s_{xy}\kappa^s_{xy} + Q^s_{yz}\gamma^s_{yz} + Q^s_{xz}\gamma^s_{xz} \end{pmatrix} \mathrm{d}x\,\mathrm{d}y. \tag{13}$$

The potential energy corresponding to the elastic foundation is defined by:

$$U_f = \frac{1}{2}\int_A \left\{K_w\left(w_b + w_s\right)^2 + K_s\left[\left(\frac{\partial\left(w_b + w_s\right)}{\partial x}\right)^2 + \right.\right.$$
$$\left.\left. + \left(\frac{\partial\left(w_b + w_s\right)}{\partial y}\right)^2\right]\right\} \mathrm{d}x\,\mathrm{d}y. \tag{14}$$

The potential energy of the plate due to the applied transverse load is given by:

$$\Omega = -\int_A q\,(w_b + w_s)\,\mathrm{d}x\,\mathrm{d}y. \tag{15}$$

where, K_w, K_s are the transverse and shear stiffness coefficients of the elastic foundation; and q is transverse applied load.

By substituting Eqs. (13)–(15) into Eq. (12), and then collecting the coefficients $(\delta u_0, \delta v_0, \delta w_b, \delta w_s)$, governing equations of the FG plate resting elastic foundation using four-variable refined theory can be obtained as follows [6, 27]:

$$\delta u_0 : \quad \frac{\partial N_x}{\partial x} + \frac{\partial N_{xy}}{\partial y} = 0, \tag{16a}$$

$$\delta v_0 : \quad \frac{\partial N_{xy}}{\partial x} + \frac{\partial N_y}{\partial y} = 0, \tag{16b}$$

$$\delta w_b : \quad \frac{\partial^2 M_x^b}{\partial x^2} + 2\frac{\partial^2 M_{xy}^b}{\partial x \partial y} + \frac{\partial^2 M_y^b}{\partial y^2} - K_w(w_b + w_s) + K_s\nabla^2(w_b + w_s) + q = 0, \tag{16c}$$

$$\delta w_s : \quad \frac{\partial^2 M_x^s}{\partial x^2} + 2\frac{\partial^2 M_{xy}^s}{\partial x \partial y} + \frac{\partial^2 M_y^s}{\partial y^2} + \frac{\partial Q_{xz}^s}{\partial x} + \frac{\partial Q_{yz}^s}{\partial y} - K_w(w_b + w_s) + K_s\nabla^2(w_b + w_s) + q = 0. \tag{16d}$$

2.3. Navier solution

In this paper, static behavior of the simply supported FG plate is solved using the Navier-type solution. The simply supported boundary conditions at ends of the FG plate are given by:

$$\begin{aligned} v_0 = w_b = w_s = N_x = M_x^b = M_x^s = 0, \quad &\text{at } x = 0,\ a, \\ u_0 = w_b = w_s = N_y = M_y^b = M_y^s = 0, \quad &\text{at } y = 0,\ b. \end{aligned} \tag{17}$$

Based on Navier's procedure, the four unknowns of the displacement field and the transverse applied load are assumed to be the double trigonometric series [28–33] satisfying the simply supported boundary conditions as follows:

$$\begin{Bmatrix} u_0 \\ v_0 \\ w_b \\ w_s \end{Bmatrix} = \sum_{m=1}^{\infty}\sum_{n=1}^{\infty} \begin{Bmatrix} u_{mn} X_m'(x) Y_n(y) \\ v_{mn} X_m(x) Y_n'(y) \\ w_{bmn} X_m(x) Y_n(y) \\ w_{smn} X_m(x) Y_n(y) \end{Bmatrix} \tag{18}$$

and

$$q = \sum_{m=1}^{\infty}\sum_{n=1}^{\infty} q_{mn} X_m(x) Y_n(y) \tag{19}$$

with

$$q_{mn} = \frac{4}{ab}\int_0^a \int_0^b q_0(x,y) X_m(x) Y_n(y)\,\mathrm{d}x\,\mathrm{d}y = \frac{16 q_0}{mn\pi^2}, \tag{20}$$

for the uniformly distributed load, where u_{mn}, v_{mn}, w_{bmn}, w_{smn} are arbitrary coefficients; and $X_m(x) = \sin(\alpha x)$, $Y_n(y) = \sin(\beta y)$ together with $\alpha = m\pi/a$, $\beta = n\pi/b$.

Substituting Eqs. (18) and (19) into Eq. (16), together with displacement components, we get linear algebraic equations as follows:

$$\begin{bmatrix} S_{11} & S_{12} & S_{13} & S_{14} \\ S_{12} & S_{22} & S_{23} & S_{24} \\ S_{13} & S_{32} & S_{33} & S_{34} \\ S_{14} & S_{24} & S_{34} & S_{44} \end{bmatrix} \times \begin{Bmatrix} u_{mn} \\ v_{mn} \\ w_{bmn} \\ w_{smn} \end{Bmatrix} = \begin{Bmatrix} 0 \\ 0 \\ q_{mn} \\ q_{mn} \end{Bmatrix}, \tag{21}$$

where

$$\begin{cases} S_{11} = A_{11}\alpha^2 + A_{66}\beta^2, \\ S_{12} = A_{12}\beta^2 + A_{66}\beta^2. \\ S_{13} = -B_{11}\alpha^2 - B_{12}\beta^2 - 2B_{66}\beta^2, \\ S_{14} = -B^s_{11}\alpha^2 - B^s_{12}\beta^2 - 2B^s_{66}\beta^2, \end{cases} \tag{22a}$$

$$\begin{cases} S_{21} = A_{66}\alpha^2 + A_{12}\alpha^2, \\ S_{22} = A_{66}\alpha^2 + A_{22}\beta^2, \\ S_{23} = -2B_{66}\alpha^2 - B_{12}\alpha^2 - B_{22}\beta^2, \\ S_{24} = -2B^s_{66}\alpha^2 - B^s_{12}\alpha^2 - B^s_{22}\beta^2, \end{cases} \tag{22b}$$

$$\begin{cases} S_{31} = -B_{11}\alpha^4 - 2B_{66}\alpha^2\beta^2 - B_{12}\alpha^2\beta^2, \\ S_{32} = -B_{12}\alpha^2\beta^2 - 2B_{66}\alpha^2\beta^2 - B_{22}\beta^4, \\ S_{33} = D_{11}\alpha^4 + 2D_{12}\alpha^2\beta^2 + 4D_{66}\alpha^2\beta^2 \\ \qquad + D_{22}\beta^4 + K_w + K_{sx}\alpha^2 + K_{sy}\beta^2, \\ S_{34} = D^s_{11}\alpha^4 + 2D^s_{12}\alpha^2\beta^2 + 4D^s_{66}\alpha^2\beta^2 \\ \qquad + D^s_{22}\beta^4 + K_w + K_{sx}\alpha^2 + K_{sy}\beta^2, \end{cases} \tag{22c}$$

$$\begin{cases} S_{41} = -B^s_{11}\alpha^4 - 2B^s_{66}\alpha^2\beta^2 - B^s_{12}\alpha^2\beta^2, \\ S_{42} = -B^s_{12}\alpha^2\beta^2 - 2B^s_{66}\alpha^2\beta^2 - B^s_{22}\beta^4, \\ S_{43} = D^s_{11}\alpha^4 + 2D^s_{12}\alpha^2\beta^2 + 4D^s_{66}\alpha^2\beta^2 \\ \qquad +D^s_{22}\beta^4 + K_w + K_{sx}\alpha^2 + K_{sy}\beta^2 \\ S_{44} = H^s_{11}\alpha^4 + 2H^s_{12}\alpha^2\beta^2 + 4H^s_{66}\alpha^2\beta^2 + H^s_{22}\beta^4 \\ \qquad +A^s_{55}\alpha^2 + A^s_{44}\beta^2 + K_w + K_{sx}\alpha^2 + K_{sy}\beta^2. \end{cases} \tag{22d}$$

Once the coefficients $(u_{mn}, v_{mn}, w_{bmn}, w_{smn})$ are determined, all involved quantities relating to the static behaviors (i.e., deflection and stress components) of the FG plate can be obtained. In the following sections, the numerical results of the static analysis of the FG plate will be presented in detail.

3. Results and discussions

Unless otherwise stated, in the next sections, a simply supported FG rectangular plate made of aluminum (as the metal) and alumina (as the ceramic) is considered. The Young's elastic moduli of the metal and the ceramic are $E_m = 70$ GPa and $E_c = 380$ GPa, respectively. The Poisson's ratio of the plate is assumed to be constant and $\nu = 0.3$. For convenience, the normalized parameters are denoted by [27]:

$$\begin{aligned} \bar{w} &= \frac{100D_0}{q_0a^4}w\left(\frac{a}{2}, \frac{b}{2}\right), \qquad \bar{z} = \frac{z}{h}, \\ \overline{\sigma}_{x(y)} &= -\frac{h^2}{q_0a^2}\sigma_{x(y)}\left(\frac{a}{2}, \frac{b}{2}, -\frac{h}{2}\right), \\ \bar{\tau}_{xy} &= \frac{h^2}{q_0a^2}\tau_{xy}\left(0, 0, -\frac{h}{2}\right), \\ \bar{\tau}_{yz} &= \frac{h}{q_0a}\tau_{yz}\left(\frac{a}{2}, 0, \frac{h}{6}\right), \\ \bar{\tau}_{xz} &= \frac{h}{q_0a}\tau_{xz}\left(0, \frac{b}{2}, 0\right), \\ K_w &= K_0\frac{E_0h^3}{a^4}, \qquad K_{sx} = \upsilon J_0\frac{E_0h^3}{a^2}, \qquad K_{sy} = \upsilon J_0\frac{E_0h^3}{b^2}, \\ E_0 &= 1 \text{ GPa}; \qquad D_0 = \frac{E_ch^3}{12(1-\upsilon^2)}. \end{aligned} \tag{23}$$

Note that K_{sx}, K_{sy} are shear stiffness coefficients of the elastic foundation in x- and y-directions.

3.1. The shift of the neutral surface from the middle surface

To investigate the shift of the neutral surface of the FG plate, in this example, two types of materials are used, they are Al/Al_2O_3 (E_m = 70 GPa, E_c = 380 GPa) and Al/ZrO_2 (E_m = 70 GPa, E_c = 200 GPa). Fig. 3 illustrates the variation of the normalized shift (z_0/h) of the neutral surface with respect to the volume fraction index.

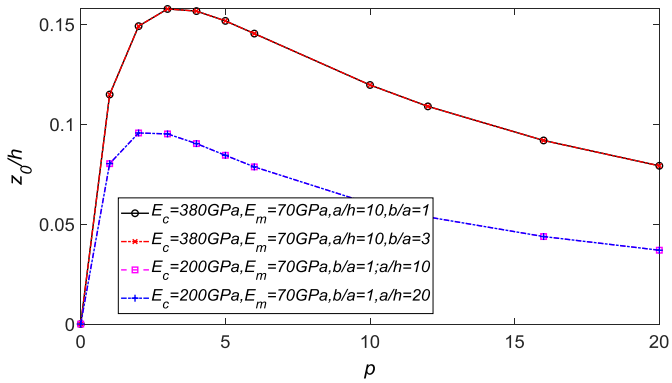

Fig. 3. The normalized shift of the neutral surface with respect to the volume fraction index

It could be noted that the shift of physical neutral surface calculated according to Eq. (2a) is independent of the dimensional parameters of the plate (a, b), however, it depends on the volume fraction index and the material properties (E_c, E_m) of the plate, and these relations are shown clearly in Fig. 3. Besides, the normalized shift is equal to zero for the case of homogeneous material (i.e., $p = 0$), and getting the maximum values when the volume fraction index $p = 2 \div 5$. The maximum values of the shift of the neutral surface are significant, which means they assume approximately 10% and 16% of the plate thickness.

3.2. Comparisons on static behaviors of the FG plate

In this section, an example is presented to compare between results of several models of displacement field (i.e., model M1, model M2, and model of the geometrical middle surface [27]) of the FG plate for static behaviors. Herein, the normalized deflection and stress components of the simply supported FG rectangular plate subjected to uniformly distributed load resting on the elastic foundation (using the physical neutral surface concept) are compared with those of Thai and Choi [27] based on the refined plate theory (without using the physical neutral surface concept), and these results are given in Table 1. The geometrical dimensions of the FG plate used are $a/h = 10$ and $a/b = 3$. As Table 1 shows, the obtained results are identical, which confirms the reliability of the present approach.

Table 1.
The normalized deflections and stress components of the FG plate resting on the elastic foundation subjected to uniformly distributed load

Power law index	K_0	J_0	Method	$\bar{w}$	$\bar{\sigma}_x$	$\bar{\sigma}_y$	$\bar{\tau}_{xy}$	$\bar{\tau}_{yz}$	$\bar{\tau}_{xz}$
$p = 5$	0	0	Ref. [27]	3.8506	0.5223	0.1785	0.2103		
			Present – M1	3.8506	0.5223	0.1785	0.2103	0.5363	0.5887
			Present – M2	3.8506	0.5223	0.1785	0.2103	0.5363	0.5887
	100	0	Ref. [27]	3.5620	0.4816	0.1633	0.1996		
			Present – M1	3.5620	0.4816	0.1633	0.1996	0.5164	0.5514
			Present – M2	3.5620	0.4816	0.1633	0.1996	0.5164	0.5514
	0	100	Ref. [27]	3.0972	0.4168	0.1394	0.1814		
			Present – M1	3.0972	0.4168	0.1394	0.1814	0.4822	0.4889
			Present – M2	3.0972	0.4168	0.1394	0.1814	0.4822	0.4889
	100	100	Ref. [27]	2.9046	0.3897	0.1294	0.1740		
			Present – M1	2.9046	0.3897	0.1294	0.1740	0.4680	0.4641
			Present – M2	2.9046	0.3897	0.1294	0.1740	0.4680	0.4641

3.3. Discussion

In this section, the FG plate using model 2 (M2) of displacement field is selected to investigate some influences of material and geometric parameters, and elastic foundation on the static behaviors of the FG plate. In the next investigations, unless otherwise stated, the geometrical dimensions of the FG plate used are $a/b = 1, a/h = 10$.

3.3.1. Effects of the volume fraction index on the stress components

To show the effects of the volume fraction index and elastic foundation on stress components, some investigations relating to normal stress components $\bar{\sigma}_x\left(\frac{a}{2}, \frac{b}{2}, z\right)$, $\bar{\sigma}_y\left(\frac{a}{2}, \frac{b}{2}, z\right)$, and shear stress $\bar{\tau}_{xy}(0, 0, z)$ and $\bar{\tau}_{xz}\left(0, \frac{b}{2}, z\right)$ with various volume fraction indexes (i.e., $p = 0, 1, 2, 5, 15$) are plotted in Figs. 4, 5, 6 and 7.

The variation of normalized stress $\overline{\sigma}_x(a/2, b/2)$ across the thickness for the FG plate not resting on elastic foundation (i.e., $K_0 = 0$, $J_0 = 0$) and resting on elastic foundation (i.e., $K_0 = 100$, $J_0 = 100$) are shown in Fig. 4a and Fig. 4b, respectively. Similarly, the variation of normalized stress $\overline{\sigma}_y(a/2, b/2)$ across the thickness of the FG plate not resting on and resting on elastic foundation are plotted in Fig. 5a and Fig. 5b.

As can be seen, the stresses vary nonlinearly through the thickness direction, except for the case of homogenous material (i.e., $p = 0$) where the stresses vary linearly. On the other hand, the stress levels of the FG plate resting on elastic foundation are smaller than those of the FG plate not resting on elastic foundation.

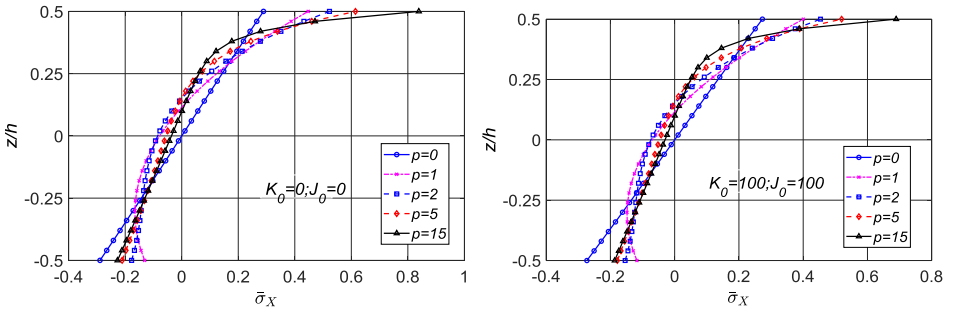

(a) without elastic foundation (b) with elastic foundation

Fig. 4. Variation of the normalized stress $\overline{\sigma}_x(a/2, b/2)$ through the thickness of the FG plate

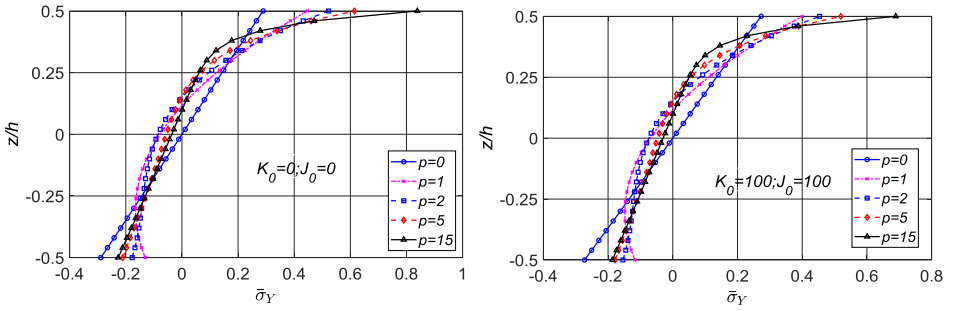

(a) without elastic foundation (b) with elastic foundation

Fig. 5. Variation of the normalized stress $\overline{\sigma}_y(a/2, b/2)$ through the thickness of the FG plate

This is because the stiffness of the plate resting on elastic foundation increases in comparison with that of the plate not resting on elastic foundation.

Fig. 6 shows the variation of the normalized shear stress $\bar{\tau}_{xy}(0, 0)$ with respect to the thickness of the FG plate. It can be observed that, due to the effect of the volume fraction index, the stresses vary nonlinearly through the thickness direction,

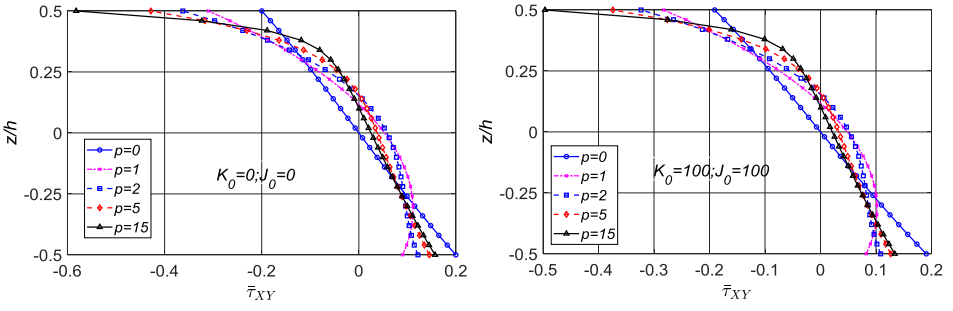

(a) without elastic foundation (b) with elastic foundation

Fig. 6. Variation of the normalized shear stress $\bar{\tau}_{xy}(0, 0)$ through the thickness of the plate

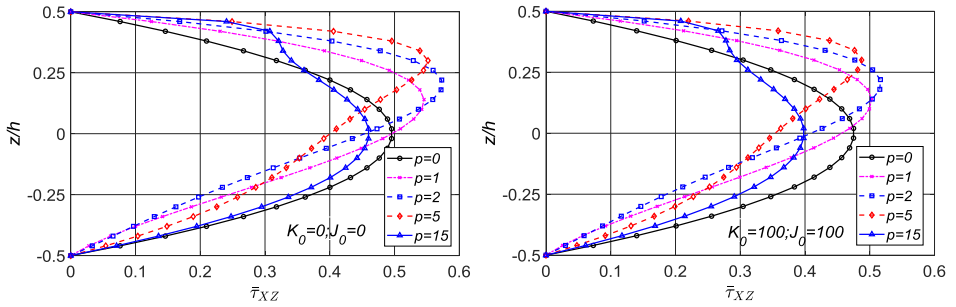

(a) without elastic foundation (b) with elastic foundation

Fig. 7. Variation of the shear stress $\bar{\tau}_{xz}(0, b/2)$ through the thickness of the FG plate

except for the case of homogeneous material (i.e., $p = 0$), in which the stresses vary linearly. Besides, the stress levels of the FG plate resting on elastic foundation are smaller than those of the FG plate not resting on elastic foundation. Next, the variation of normalized shear stress $\bar{\tau}_{xz}(0, b/2)$ with respect to the plate thickness with some volume fraction indexes is plotted in Fig. 7. It can be seen that the shear stresses satisfy the zeros conditions at the top and the bottom surfaces of the FG plate. In the case of homogeneous material (i.e., $p = 0$), the shear stresses $\bar{\tau}_{xz}(0, b/2)$ are the parabolic curves. Besides, the maximum values of the shear stress for the case of isotropic material occur at the geometrical middle surface ($z = 0$), however, the in other cases they do not occur at the middle surface of the FG plate, as shown in Fig. 7.

3.3.2. Effects of the geometrical parameters on the plate deflection

To show the effects of the geometrical parameters on the normalized deflections of the FG plate, two cases, the results of the deflection at the center of the plate corresponding to the a/b and a/h ratios are investigated. The influences of the a/b ratio on the normalized deflection of the FG plate are illustrated in Fig. 8, whereas the effects of a/h ratio on the normalized deflection are shown in Fig. 9.

As Figs. 8 and 9 show, in both two cases, the normalized deflections of FG plate decrease when the geometrical parameters a/b and a/h increase. The normalized deflections of the FG plate decrease sharply as the geometrical parameters (a/b, a/h) are small, as shown in the figures. It can be said that the deflection of the FG plate is sensitive to the small changes in geometrical parameters (a/b, a/h).

By contrast, from Figs. 8 and 9, one can note that the normalized deflections of the FG plate generally increase when the volume fraction indexes increase. This phenomenon is due to the overall stiffness of the FG plate decrease when the ceramic content in the FG plate decreases (i.e., volume fraction indexes rise). Moreover, comparisons between results from Figs. 8a and 8b, and between results from Figs. 9a and 9b, show that the elastic foundation leads to decreasing in

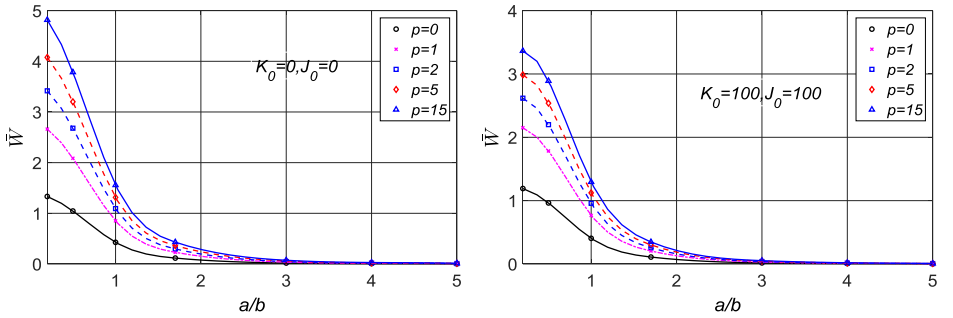

(a) without elastic foundation (b) with elastic foundation

Fig. 8. The effect of a/b ratio on the normalized deflection at the center of the FG plate

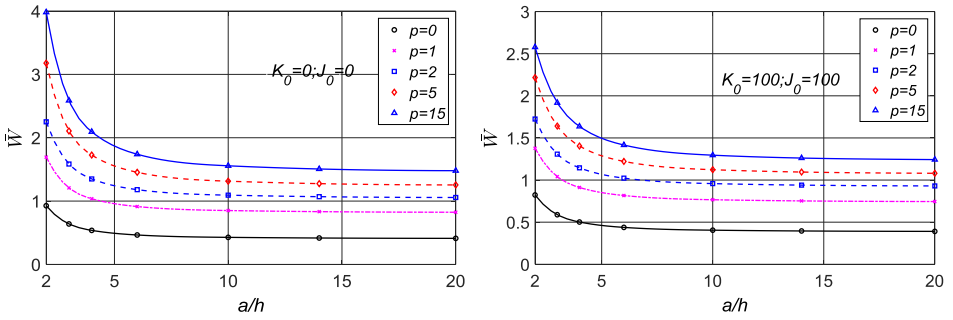

(a) without elastic foundation (b) with elastic foundation

Fig. 9. The effect of a/h ratio on the normalized deflection at the center of the FG plate

deflections of the FG plate. It is because the elastic foundation is found to enhance the overall stiffness of the plate.

4. Conclusions

In this paper, a study on static behaviors (i.e., deflection and stress components) of the simply supported functionally graded plate resting on the elastic foundation based on the four-variable refined theory and the physical neutral surface concept is presented using the Navier' procedure. In the numerical results, comparisons of static behaviors between several models of displacement field are illustrated, and several numerical investigations relating to the effects of parameters (volume fraction index, dimension ratios, and elastic foundation) on the results of the FG plate are given.

Based on numerical investigations, some key points can be given: (i) The maximum values of the normalized shift of the neutral surface of the FG plate are significant in comparison with the plate thickness. (ii) The results of the static behaviors based on the physical neutral surface concept (both M1 and M2 models)

of the FG plate exhibit insignificant differences in comparison with those of the geometrical middle surface. (iii) The normalized deflections of the functionally graded plate increase when the volume fraction indexes increase, due to decrease in the stiffness of the FG plate as the ceramic content decreases. (iv) The small geometrical ratios a/b and a/h are sensitive to the deflection of the FG plate, and the deflection decreases sharply with the small a/b and a/h ratios. (v) The effect of the elastic foundations leads to decreasing in the defection and the normal stresses of the FG plate, which is due to heightening of the overall stiffness of the FG plate resting on elastic foundation.

Besides, based on the present study, some potential research topics relating to nonlinear analysis of the FG plate and shell structures using the physical neutral surface concept can be investigated in future works.

Acknowledgements

This work is funded by the National University of Civil Engineering (Vietnam), the project 25-2020/KHXD-TD. The authors are grateful for the financial support.

We sincerely thank Reviewers for constructive comments which led to improvement of the article.

Manuscript received by Editorial Board, September 01, 2020;
final version, December 29, 2020.

References

[1] J.N. Reddy and C.D. Chin. Thermomechanical analysis of functionally graded cylinders and plates. *Journal of Thermal Stresses*, 21(6):593–626, 1998. doi: 10.1080/01495739808956165.

[2] S-H. Chi and Y-L.Chung. Mechanical behavior of functionally graded material plates under transverse load – Part I: Analysis. *International Journal of Solids and Structures*, 43(13):3657–3674, 2006. doi: 10.1016/j.ijsolstr.2005.04.011.

[3] V-L. Nguyen and T-P. Hoang. Analytical solution for free vibration of stiffened functionally graded cylindrical shell structure resting on elastic foundation. *SN Applied Sciences*, 1(10):1150, 2019. doi: 10.1007/s42452-019-1168-y.

[4] A.M. Zenkour and N.A. Alghamdi. T hermoelastic bending analysis of functionally graded sandwich plates. *Journal of Materials Science*, 43(8):2574–2589, 2008. doi: 10.1007/s10853-008-2476-6.

[5] S.A. Sina, H.M. Navazi, and H. Haddadpour. An analytical method for free vibration analysis of functionally graded beams. *Materials & Design*, 30(3):741–747, 2009. doi: 10.1016/j.matdes.2008.05.015.

[6] I. Mechab, H.A. Atmane, A. Tounsi, H.A. Belhadj, E.A. Adda Bedia. A two variable refined plate theory for the bending analysis of functionally graded plates. *Acta Mechanica Sinica*, 26(6):941–949, 2010. doi: 10.1007/s10409-010-0372-1.

[7] M.T. Tran, V.L. Nguyen, and A.T. Trinh. Static and vibration analysis of cross-ply laminated composite doubly curved shallow shell panels with stiffeners resting on Winkler–Pasternak elastic foundations. *International Journal of Advanced Structural Engineering*, 9(2):153–164, 2017. doi: 10.1007/s40091-017-0155-z.

[8] A. Gholipour, H. Farokhi, and M.H. Ghayesh. In-plane and out-of-plane nonlinear size-dependent dynamics of microplates. *Nonlinear Dynamics*, 79(3):1771–1785, 2015. doi: 10.1007/s11071-014-1773-7.

[9] M.T. Tran, V.L. Nguyen, S.D. Pham, and J. Rungamornrat. Vibration analysis of rotating functionally graded cylindrical shells with orthogonal stiffeners. *Acta Mechanica*, 231:2545–2564, 2020. doi: 10.1007/s00707-020-02658-y.

[10] S-H. Chi and Y-L. Chung. Mechanical behavior of functionally graded material plates under transverse load – Part II: Numerical results. *International Journal of Solids and Structures*, 43(13):3675–3691, 2006. doi: 10.1016/j.ijsolstr.2005.04.010.

[11] S. Hosseini-Hashemi, H.R.D Taher, H. Akhavan, and M. Omidi. Free vibration of functionally graded rectangular plates using first-order shear deformation plate theory. *Applied Mathematical Modelling*, 34(5):1276–1291, 2010. doi: 10.1016/j.apm.2009.08.008.

[12] M.S.A. Houari, S. Benyoucef, I. Mechab, A. Tounsi, and E.A. Adda Bedia. Two-variable refined plate theory for thermoelastic bending analysis of functionally graded sandwich plates. *Journal of Thermal Stresses*, 34(4):315–334, 2011. doi: 10.1080/01495739.2010.550806.

[13] M.Talha and B.N. Singh. Static response and free vibration analysis of FGM plates using higher order shear deformation theory. *Applied Mathematical Modelling*, 34(12):3991–4011, 2010. doi: 10.1016/j.apm.2010.03.034.

[14] H-T. Thai and S-E. Kim. A simple higher-order shear deformation theory for bending and free vibration analysis of functionally graded plates. textitComposite Structures, 96:165–173, 2013. doi: 10.1016/j.compstruct.2012.08.025.

[15] A. Chikh, A. Tounsi, H. Hebali, and S.R. Mahmoud. Thermal buckling analysis of cross-ply laminated plates using a simplified HSDT. *Smart Structures and Systems*, 19(3):289–297, 2017. doi: 10.12989/sss.2017.19.3.289.

[16] H.H. Abdelaziz, M.A.A. Meziane, A.A. Bousahla, A. Tounsi, S.R. Mahmoud, and A.S. Alwabli. An efficient hyperbolic shear deformation theory for bending, buckling and free vibration of FGM sandwich plates with various boundary conditions. *Steel and Composite Structures*, 25(6):693–704, 2017. doi: 10.12989/scs.2017.25.6.693.

[17] D-G. Zhang, Y-H. Zhou. A theoretical analysis of FGM thin plates based on physical neutral surface. *Computational Materials Science*, 44(2):716–720, 2008. doi: 10.1016/j.commatsci.2008.05.016.

[18] A.A. Bousahla, M.S.A. Houari, A. Tounsi A, E.A. Adda Bedia. A novel higher order shear and normal deformation theory based on neutral surface position for bending analysis of advanced composite plates. *International Journal of Computational Methods*, 11(06):1350082, 2014. doi: 10.1142/S0219876213500825.

[19] Y. Liu, S. Su, H. Huang, and Y. Liang. Thermal-mechanical coupling buckling analysis of porous functionally graded sandwich beams based on physical neutral plane. *Composites Part B: Engineering*, 168:236–242, 2019. doi: 10.1016/j.compositesb.2018.12.063.

[20] D-G. Zhang. Thermal post-buckling and nonlinear vibration analysis of FGM beams based on physical neutral surface and high order shear deformation theory. *Meccanica*, 49(2):283–293, 2014. doi: 10.1007/s11012-013-9793-9.

[21] D-G. Zhang. Nonlinear bending analysis of FGM beams based on physical neutral surface and high order shear deformation theory. *Composite Structures*, 100:121–126, 2013. doi: 10.1016/j.compstruct.2012.12.024.

[22] H-T. Thai and B. Uy. Levy solution for buckling analysis of functionally graded plates based on a refined plate theory. *Proceedings of the Institution of Mechanical Engineers, Part C: Journal of Mechanical Engineering Science*, 227(12):2649–2664, 2013. doi: 10.1177/0954406213478526.

[23] Y. Khalfi, M.S.A. Houari, and A. Tounsi. A refined and simple shear deformation theory for thermal buckling of solar functionally graded plates on elastic foundation. *International Journal of Computational Methods*, 11(05):1350077, 2014. doi: 10.1142/S0219876213500771.

[24] H. Bellifa, K.H. Benrahou, L. Hadji, M.S.A. Houari, and A. Tounsi. Bending and free vibration analysis of functionally graded plates using a simple shear deformation theory and the concept the neutral surface position. *Journal of the Brazilian Society of Mechanical Sciences and Engineering*, 38(1):265–275, 2016. doi: 10.1007/s40430-015-0354-0.

[25] H. Shahverdi and M.R. Barati. Vibration analysis of porous functionally graded nanoplates. *International Journal of Engineering Science*, 120:82–99, 2017. doi: 10.1016/j.ijengsci.2017.06.008.

[26] R.P. Shimpi and H.G. Patel. A two variable refined plate theory for orthotropic plate analysis. *International Journal of Solids and Structures*, 43(22-23):6783–6799, 2006. doi: 10.1016/j.ijsolstr.2006.02.007.

[27] H-T. Thai and D-H. Choi. A refined plate theory for functionally graded plates resting on elastic foundation. *Composites Science and Technology*, 71(16):1850–1858, 2011. doi: 10.1016/j.compscitech.2011.08.016

[28] M.H. Ghayesh. Viscoelastic nonlinear dynamic behaviour of Timoshenko FG beams. *The European Physical Journal Plus*, 134(8):401, 2019. doi: 10.1140/epjp/i2019-12472-x.

[29] M.H. Ghayesh. Nonlinear oscillations of FG cantilevers. *Applied Acoustics*, 145:393–398, 2019. doi: 10.1016/j.apacoust.2018.08.014.

[30] M.H. Ghayesh. Dynamical analysis of multilayered cantilevers. *Communications in Nonlinear Science and Numerical Simulation*, 71:244–253, 2019. doi: 10.1016/j.cnsns.2018.08.012.

[31] M.H. Ghayesh. Mechanics of viscoelastic functionally graded microcantilevers. *European Journal of Mechanics - A/Solids*, 73:492–499, 2019. doi: 10.1016/j.euromechsol.2018.09.001.

[32] M.H. Ghayesh. Dynamics of functionally graded viscoelastic microbeams. *International Journal of Engineering Science*, 124:115–131, 2018. doi: 10.1016/j.ijengsci.2017.11.004.

[33] A.T. Trinh, M.T. Tran, H.Q. Tran, and V.L. Nguyen. Vibration analysis of cross-ply laminated composite doubly curved shallow shell panels with stiffeners. *Vietnam Journal of Science and Technology*, 55(3):382–392, 2017. doi: 10.15625/2525-2518/55/3/8823.